OPEN ACCESS Freely available online

PLOS ONE

Synergistic Removal of Pb(II), Cd(II) and Humic Acid by Fe_3O_4@Mesoporous Silica-Graphene Oxide Composites

Yilong Wang[1], Song Liang[2], Bingdi Chen[1], Fangfang Guo[1], Shuili Yu[2], Yulin Tang[2]*

1 The Institute for Biomedical Engineering and Nano Science, Tongji University School of Medicine, Shanghai, P. R. China, **2** State Key Laboratory of Pollution Control and Resource Reuse, College of Environmental Science and Engineering, Tongji University, Shanghai, P. R. China

Abstract

The synergistic adsorption of heavy metal ions and humic acid can be very challenging. This is largely because of their competitive adsorption onto most adsorbent materials. Hierarchically structured composites containing polyethylenimine-modified magnetic mesoporous silica and graphene oxide (MMSP-GO) were here prepared to address this. Magnetic mesoporous silica microspheres were synthesized and functionalized with PEI molecules, providing many amine groups for chemical conjugation with the carboxyl groups on GO sheets and enhanced the affinity between the pollutants and the mesoporous silica. The features of the composites were characterized using TEM, SEM, TGA, DLS, and VSM measurements. Series adsorption results proved that this system was suitable for simultaneous and efficient removal of heavy metal ions and humic acid using MMSP-GO composites as adsorbents. The maximum adsorption capacities of MMSP-GO for Pb(II) and Cd (II) were 333 and 167 mg g^{-1} caculated by Langmuir model, respectively. HA enhances adsorption of heavy metals by MMSP-GO composites due to their interactions in aqueous solutions. The underlying mechanism of synergistic adsorption of heavy metal ions and humic acid were discussed. MMSP-GO composites have shown promise for use as adsorbents in the simultaneous removal of heavy metals and humic acid in wastewater treatment processes.

Citation: Wang Y, Liang S, Chen B, Guo F, Yu S, et al. (2013) Synergistic Removal of Pb(II), Cd(II) and Humic Acid by Fe_3O_4@Mesoporous Silica-Graphene Oxide Composites. PLoS ONE 8(6): e65634. doi:10.1371/journal.pone.0065634

Editor: Stephen J. Johnson, University of Kansas, United States of America

Received January 16, 2013; **Accepted** April 25, 2013; **Published** June 11, 2013

Funding: This work was supported by National Natural Science Foundation of China (numbers 51003077, 51173135, 21007048), Nano-tech Foundation of Shanghai (11 nm0506100), and the Fundamental Research Funds for the Central Universities. The funders had no role in study design, data collection and analysis, decision to publish, or preparation of the manuscript.

Competing Interests: The authors have declared that no competing interests exist.

* E-mail: tangyulin@tongji.edu.cn

Introduction

Heavy metal ions and humic acid (HA) in underground water pose a severe threat to public health and ecological systems.[1–3] A great deal of effort has been made to develop effective adsorbents with different chemical compositions, microstructures, and surface functionalities for the removal of heavy metal ions and organic pollutants from water.[4–9] In this way, the development of adsorbents with high adsorption capacity, low toxicity, and efficient separation has attracted considerable interest. [10,11].

In the past decades, silica-based mesoporous materials, which are robust inorganic solids, have shown good potential in water treatment applications due to their large specific surface area (200–1500 m^2 g^{-1}) and accessible surface functionalization. [12,13] Mesoporous silica groups containing amino and thiol groups have been extensively used to accumulate the metal ions from aqueous solutions.[14–20] Recently, magnetic nanoparticles have been introduced in mesoporous silica adsorbents, contributing to direct enhancement of the adsorption of metal ions and possible recovery by magnetic separation [21–23].

Recently, the development of bifunctionalized adsorbents capable of enabling simultaneous removal of two kinds of environmental pollutants has become an emerging frontier in the field of water treatment. [24] However, synergistic adsorption of heavy metal ions and humic acid molecules is still a challenge because of their competitive adsorption onto most adsorbents.[25–27] To the best of our knowledge, there have been few studies that have evaluated the use of functionalized magnetic mesoporous silica and graphene oxide in the synergistic adsorption of two kind of pollutants. The high surface-to-volume ratio and surface functionalities of the graphene oxide (GO) and PEI-grafted magnetic mesoporous silica (MMSP) microspheres can be both used to this effect. The addition of GO can further improve the colloidal stability of the MMSP.

Herein, we report a facile method for preparation of magnetic mesoporous silica-graphene oxide (MMSP-GO) composites and describe our investigation of the synergistic adsorption of HA and heavy metal ions, specifically Pb(II) and Cd(II). First, the magnetic mesoporous silica microspheres were synthesized and functionalized with PEI molecules, followed by chemical conjugation with the carboxyl groups on GO sheets. The functionalization of the mesoporous silica microspheres containing PEI molecules was found to both facilitate the adsorption of HA and provide sites for chemical reaction with graphene oxide sheets. The adsorption isotherm of Pb(II) and Cd(II) by MMSP-GO composites were studied. And the underlying mechanism of synergistic adsorption of heavy metal ions and humic acid were discussed. The magnetic cores of MMSP microspheres were also embedded to facilitate easy separation using magnetic fields.

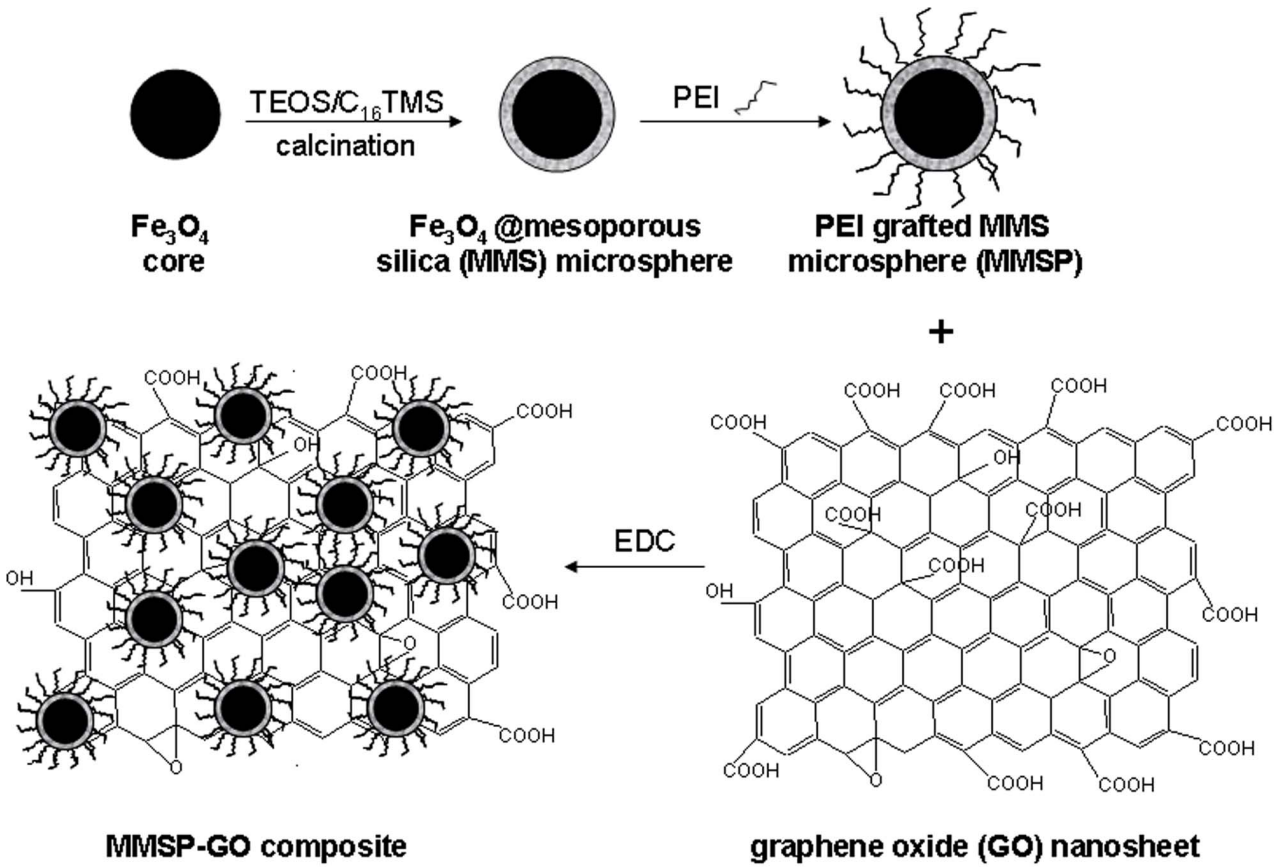

Figure 1. Scheme of the preparation pathway. Schemetic illustration of pathway for preparation of polyethylenimine-modified magnetic mesoporous silica and graphene oxide (MMSP-GO) composites.
doi:10.1371/journal.pone.0065634.g001

Experimental procedures

2.1. Materials

$Pb(NO_3)_2$, $CdCl_2{\cdot}2.5H_2O$, iron (III) chloride hydrate ($FeCl_3{\cdot}6H_2O$), sodium acetate, ethylene glycol, ammonium hydroxide (NH_4OH, 28 wt%), and hydrochloric acid (37 wt% aqueous solution) were purchased from Shanghai Reagent Company (China). Tetraethoxysilane was purchased from Sigma-Aldrich (U.S.). Hexadecyltrimethoxysilane ($C_{16}TMS$) and polyethyleneimide (PEI, 99%, Mw = 1800) were purchased from Alfa Aesar (U.S.). Humic acid was purchased from Aldrich Chemical Company (China) and treated using the method described in our previous experiment. [28] Graphene oxide was purchased from Nanjing XF Nano Company (China). All these reagents were used without further purification. The deionized (DI) water used for the preparation of reagents was purified by Millipore reverse osmosis (RO).

2.2. Instruments

The TEM samples were dispersed in DI water and dried onto carbon-coated copper grids before examination. Transmission electron microscope (TEM) images were obtained with a Philips Tecnai 20 transmission electron microscope. Scanning electron microscope (SEM) images were taken using a JEOL SM4800 scanning electron microscope. FTIR spectra were obtained with a Bruker Tensor 27. The TGA data was obtained with a thermogravimetric analyzer (NETZSCH TG209) conducted under nitrogen atmosphere from ambient to 1173 K with the rate of heating at 283 K min^{-1}. The magnetic properties were measured at room temperature using a Vibrating Sample Magnetometer (VSM 7407, Lake Shore, USA). The surface zeta potentials of the microspheres were measured using a DLS Particle Size analyzer (Zetasizer Nano-ZS, Malvern, UK.).

The concentrations of total Cd (II) and Pb (II) were determined by an ICP-AES (ICP-optima 2001DV, Perkin-Elmer, USA). Humic acid was determined using a UV-vis spectrophotometer at 254 nm wavelength. The pH of the solutions was measured using a pH meter (pHS-3C model, Leici, China).

2.3. Preparation of MMSP-GO Composites

2.3.1. Synthesis of PEI-modified magnetic mesoporous silica microspheres. *Synthesis of Fe_3O_4 microspheres.* The magnetic microspheres were prepared using a solvothermal reaction. [29] Then 2.16 g of sodium acetate and 0.86 g of $FeCl_3{\cdot}6H_2O$ were dissolved in 30 mL of ethylene glycol under vigorous magnetic stirring. The homogeneous yellow solution was transferred to the Teflon-lined stainless-steel autoclave and heated to 200°C for nearly 8 h. After that, the autoclave was cooled to room temperature. The products were washed three times with ethanol and DI water and redispersed into DI water for use.

Synthesis of core-shell structure magnetic mesoporous silica composite microspheres. First, 4 mL of Fe_3O_4 aqueous dispersion (about 100 mg mL^{-1}) was treated with 0.1 M HCl aqueous solution under sonication for 20 min. The treated Fe_3O_4 microspheres were dispersed in the mixture of ethanol and water (v/v = 70/30) for a while. Ammonium hydroxide was added to adjust pH value

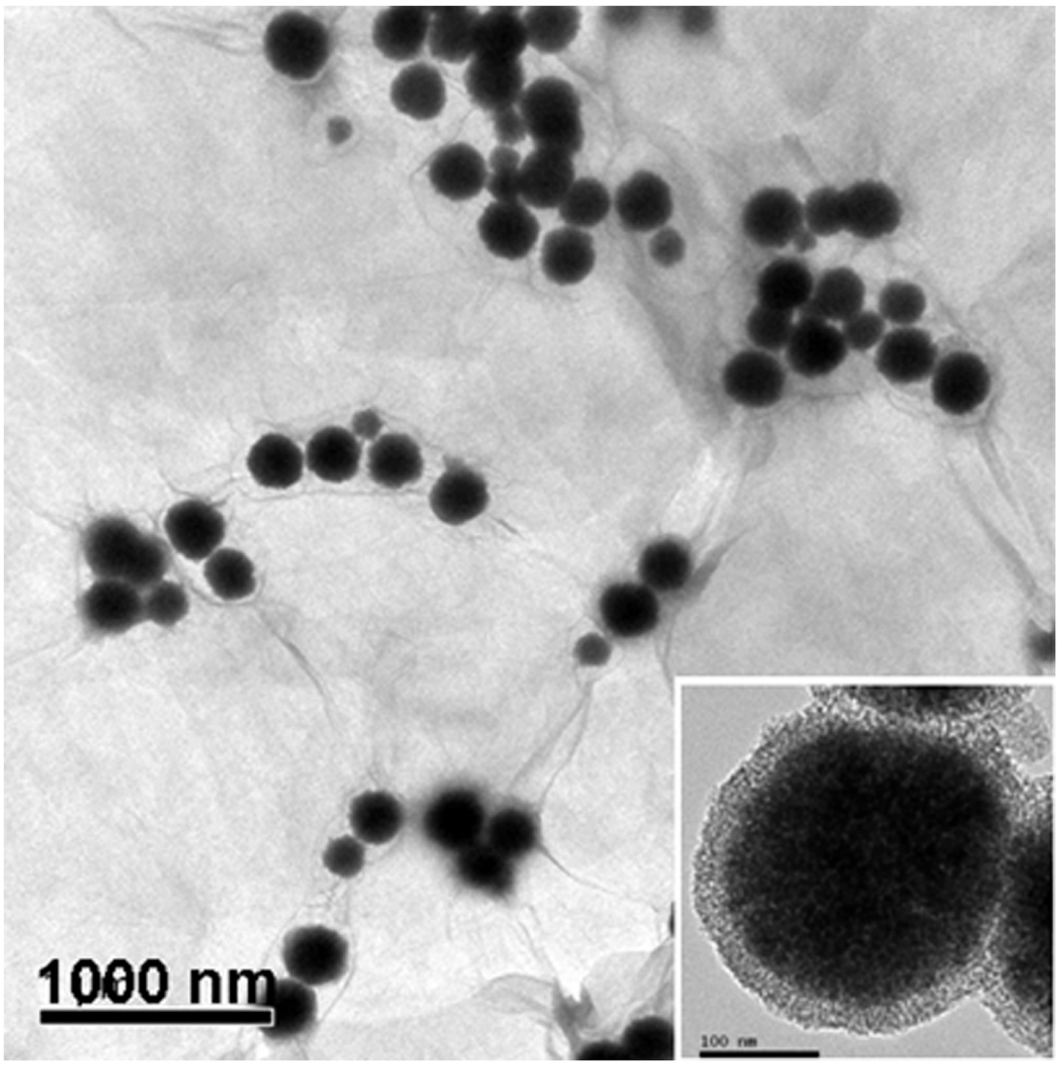

Figure 2. TEM images of the composites. TEM image of polyethylenimine-modified magnetic mesoporous silica and graphene oxide (MMSP-GO) composites (inset is the enlarged TEM image of an individual Fe_3O_4@mesoporous silica microsphere on the GO sheet).
doi:10.1371/journal.pone.0065634.g002

of the dispersion to about 9.5. Then 0.12 mL of TEOS was poured into the reactor with vigorous stirring at room temperature. The reaction lasted for about 24 h. The extra reactants were washed four times with ethanol and removed from Fe_3O_4@SiO2 microspheres. Then 150 mL of the mixture of ethanol and DI water (v/v = 88/12) was treated with 7.2 mL of ammonium hydroxide. Then 5 mL of ethanol solution of TEOS and C_{16}TMS (molar ratio of 4.7:1) was dropped into the reaction system at the rate of one drop every 10 seconds. The mixture was stirred at constant temperature for 6 h and then the reaction was stopped. The product was washed twice with ethanol and DI water and then calcinated at 550°C for 6 h, producing magnetic mesoporous silica composite microspheres.

Surface modification of magnetic mesoporous silica composite microspheres with PEI molecules. In 35 mL of DI water, 20 mg of as-synthesized magnetic mesoporous silica microspheres was dispersed under sonication. Then 30 mg of PEI (Fw = 1800) was added to the aqueous dispersion with vigorous mechanical stirring and sonication. After 30 min, the resulting MMSP were washed three times with DI water.

2.3.2. Synthesis of MMSP-GO composites. In a 50 mL centrifuge tube, 20 mg of GO sheets were dispersed in 30 mL of DI water with 1 h sonication. Into this yellow-brown homogeneous dispersion, 0.080 mL of newly-produced EDC aqueous solution at a concentration of 4.0 mg mL^{-1} was added. This mixture was vortexed for 8 min. Then 2 mg of PEI functionalized magnetic mesoporous silica microspheres were introduced. The reaction lasted for 2.5 h in an end-over-end reactor and the final products were purified by washing three times with DI water, producing MMSP-GO composites.

2.4. Adsorption of Pb(II)/Cd(II) and HA

Batch experiments were employed to evaluate Pb(II) and Cd(II) or HA adsorption characteristics under various conditions. All the adsorption experiments were conducted at room temperature (25±1°C). The average values of triplicate measurements were reported and all standard errors were smaller than 5%.

The batch adsorption procedure consisted of (a) distributing 1.0 mg of MMSP-GO or MMSP through 10 mL water solution containing selected concentrations of Pb(II) and Cd(II) in a series of 20 mL glass tubes; (b) adjusting the pH to 2.0–9.0 using 0.1 M

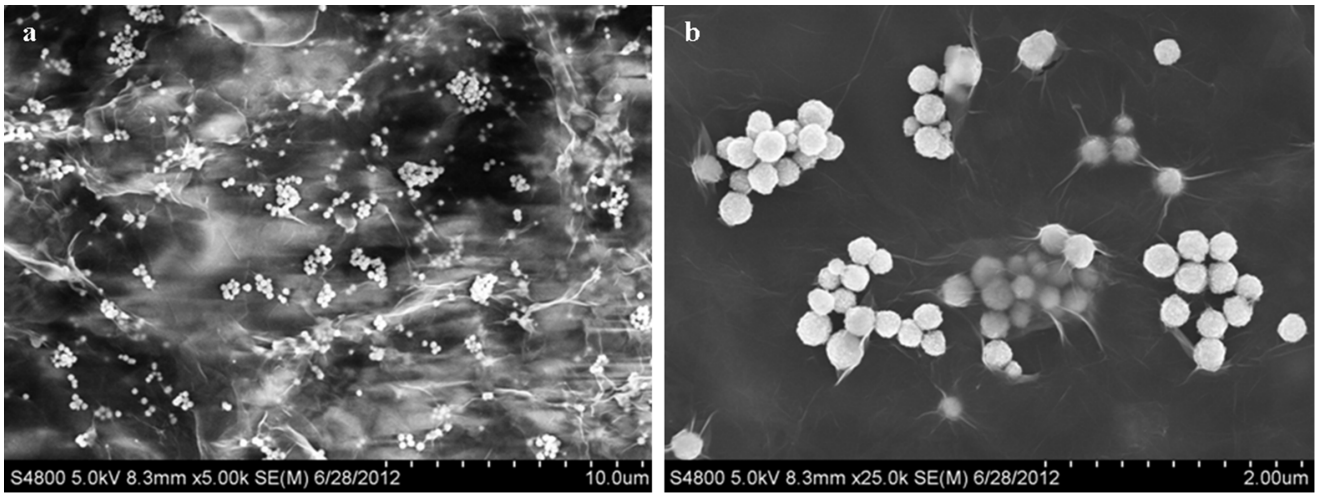

Figure 3. SEM images of the composites. SEM images of polyethylenimine-modified magnetic mesoporous silica and graphene oxide (MMSP-GO) composites.
doi:10.1371/journal.pone.0065634.g003

stock of HNO_3 and NaOH solution; (c) adding HA stock solution to each of the tubes to specific preselected concentrations; (d) sealing and shaking all tubes in an incubator at 150 rpm; (e) separating the suspension using an external magnetic field; (f) detection of the residual Pb(II) and Cd(II) concentrations with ICP-AES and detection of the residual concentration of HA with an UV-vis spectrophotometer; (g) calculation of the amounts of heavy metal and HA adsorbed using Eq. (1):

$$q_t = \frac{(C_0 - C_t)V}{M} \quad (1)$$

Here q_t (mg/g) is the amount of heavy metal or HA adsorbed at time t, C_0 (mg L^{-1}) is the initial heavy metal or HA concentration. C_t (mg L^{-1}) is the heavy metal or HA concentration at time t. V (mL) is the volume of heavy metal or HA solution, and M (g) is the adsorbent mass.

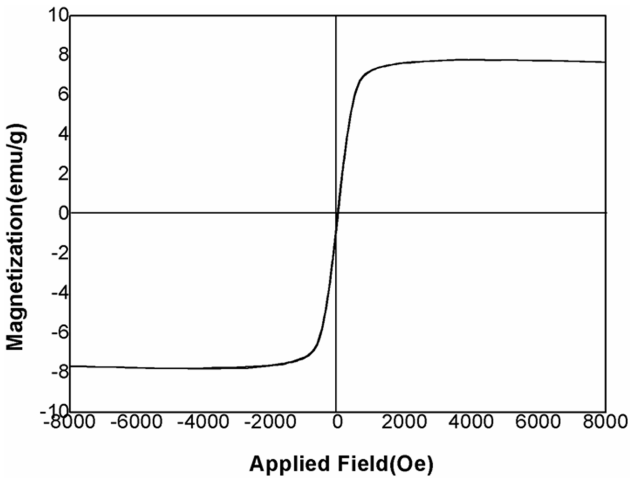

Figure 4. Magnetic property of the composites. Magnetic property of the polyethylenimine-modified magnetic mesoporous silica and graphene oxide (MMSP-GO) composites.
doi:10.1371/journal.pone.0065634.g004

Results and Discussion

3.1. Material Characterizations

The typical synthesis of the MMSP-GO composites is shown schematically in Figure 1. Fe_3O_4@mesoporous silica (MMS) core-shell microspheres were first prepared using standard methods of mesoporous silica shell formation via a sol-gel process based on the magnetic microspheres obtained through a solvothermal reaction. [29] C_{16}TMS, a coupling agent, was used as the porogen during the silica coating on the magnetic cores, which could be easily removed by calcination. Then monodispersed MMS core-shell microspheres with regular mesoporous silica shells were produced. In order to connect the magnetic mesoporous composites to the graphene oxide sheets, PEI branched molecules were used to modify the surface of the mesoporous microspheres by electrostatic adsorption. [30] The dramatically change in the surface potential of the mesoporous microspheres from −15 mV to +37 mV under the neutral conditions proved that the modification was successful. Next, the formation of MMSP-GO composites was carried out by

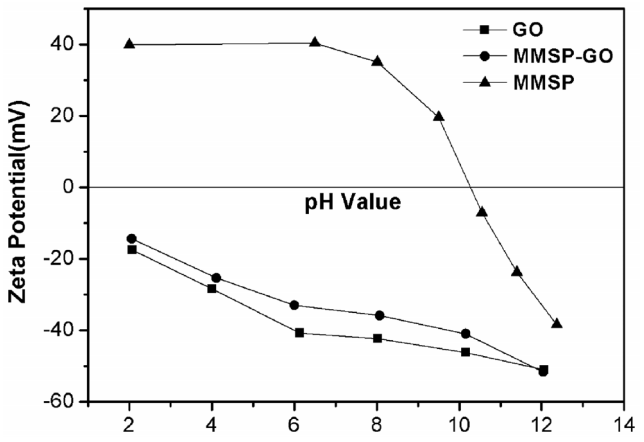

Figure 5. pH-zeta potential relation curves. pH-zeta potential relation curves of polyethylenimine-modified magnetic mesoporous silica and graphene oxide (MMSP-GO) composites, MMSP microspheres, and GO nanosheets, respectively.
doi:10.1371/journal.pone.0065634.g005

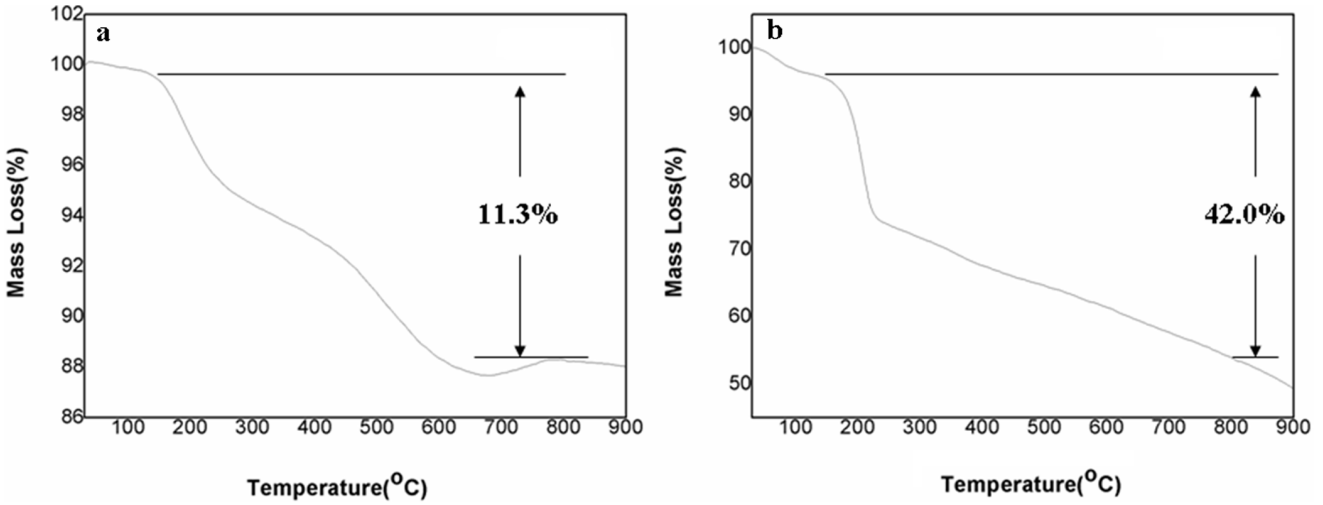

Figure 6. TG analysis curves. TG analysis of (a) polyethylenimine-modified magnetic mesoporous silica and graphene oxide (MMSP-GO) composites and (b) polyethylenimine-modified magnetic mesoporous silica microspheres.
doi:10.1371/journal.pone.0065634.g006

chemical reaction of MMSP and original GO nanosheets in the presence of 1-ethyl-3-(3-dimethyaminopropyl) carbodiimide (EDC) (Figure 1). In this case, PEI molecules played bilateral roles one of them serving as the binding bridge for conjugation and the other to improve the adsorption affinity of the MMSP microspheres to the pollutant matter. [28].

Figure 2 shows a TEM image of MMSP-GO composites. The monodispersed MMSP microspheres were distributed on the GO surface. Some microspheres adhered to each other, leaving most of the GO surface exposed. There was little aggregation or multilayer accumulation of the MMSP microspheres, implying good connections between the microspheres and the GO sheets. The average diameter of the MMSP microspheres was 260 nm. The microstructures of the MMSP microspheres were shown in the inset of Figure 2. There was an obvious mesoporous silica shell on the Fe_3O_4 core. The loading density of MMSP microspheres on the GO surface could be well controlled maintaining the balance between strong adsorption properties and magnetic resonance.

Figure 3 shows SEM images of MMSP-GO composites at different magnifications. In Figure 3a, the low-magnification SEM image indicates that the MMSP microspheres were distributed homogeneously across the whole surface of the GO. As shown, the MMSP microspheres were firmly anchored on both sides of the wrinkled GO nanosheets (Figure 3b). These GO layers may play a critical role in preventing MMSP microspheres from aggregating in solution.

Figure 4 gives magnetic hysteresis loops for MMSP-GO composites measured at 300 K. The profile of the magnetization curve of the MMSP-GO composites showed their typical super-paramagnetic properties. The saturation magnetization of the MMSP-GO was 7.5 emu g^{-1}, which ensured effective magnetic separation after adsorption equilibrium.

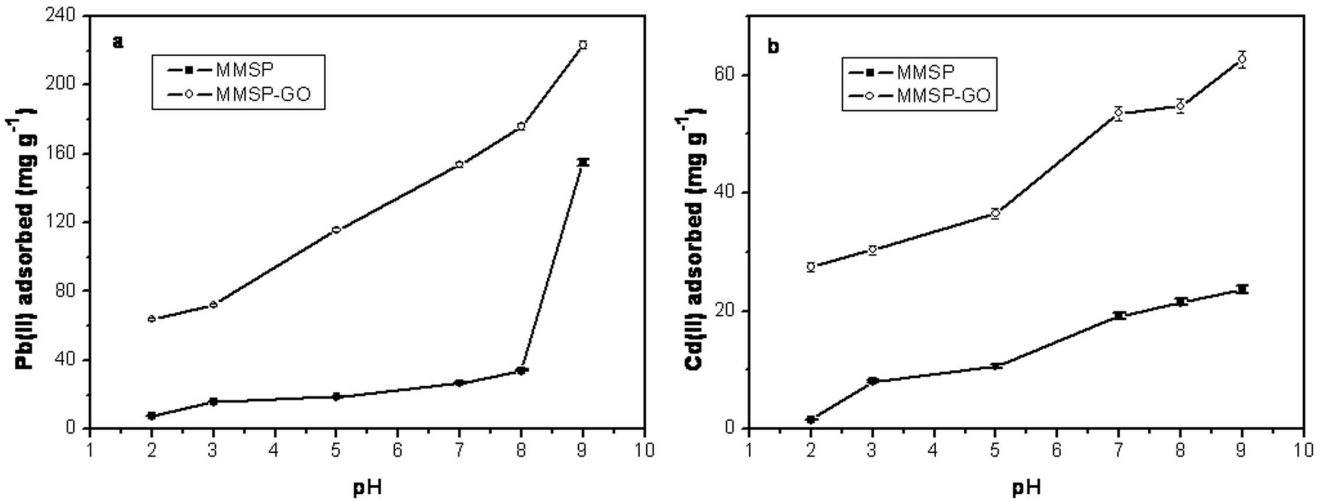

Figure 7. Comparison of adsorptive capacities of heavy metal ions by different materials. a. Effects of pH on adsorption of Pb(II) by polyethylenimine-modified magnetic mesoporous silica (MMSP) and polyethylenimine-modified magnetic mesoporous silica and graphene oxide (MMSP-GO) (Initial concentrations: 20 mg L^{-1}; adsorbent loading: 100 mg L^{-1}); b. Effects of pH on adsorption of Cd(II) by MMSP and MMSP-GO (Initial concentrations: 20 mg L^{-1}; adsorbent loading: 100 mg L^{-1}).
doi:10.1371/journal.pone.0065634.g007

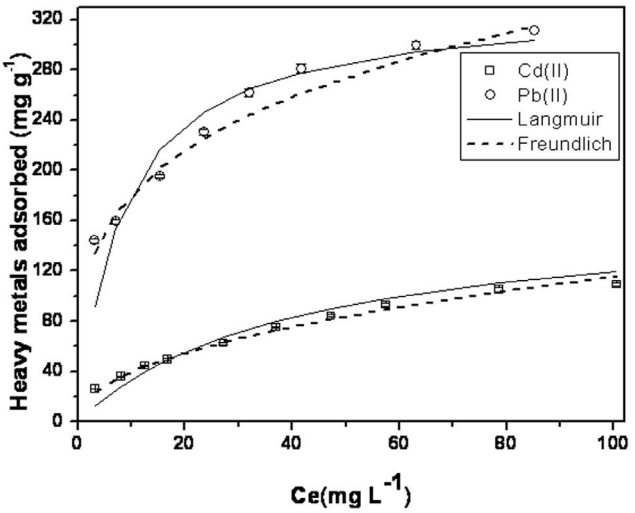

Figure 8. Pb(II) and Cd(II) adsorption isotherms on MMSP-GO. Pb(II) and Cd(II) adsorption isotherms on MMSP-GO (adsorbent loading: 100 mg L^{-1}; pH: 7.1; contact time: 24 h). The solid lines are Langmuir model simulation, and the dotted lines are Freundlich model simulation.
doi:10.1371/journal.pone.0065634.g008

Zeta potentials of MMSP-GO composites and corresponding two components of GO and MMSP as a function of solution pH are shown in Figure 5. The point of zero charge (pH_{pzc}) of MMSP was 10.4 because of the existence of large numbers of PEI molecules. Points of zero charge (pH_{pzc}) of MMSP-GO composites and GO nanosheets approached 1.0. This was because both of them had many oxygen-containing groups on their surfaces. This showed that a majority of the functional groups of GO were still present after the formation of the composites.

To calculate the composition partition of microspheres to GO nanosheets, we performed TGA analysis of the MMSP-GO composites and MMSP microspheres (Figure 6). The big mass loss of the composites (42.0%) at temperature between 150 to 800°C was due to removal of oxygen-containing functional groups of GO and PEI molecules on MSP microspheres. The loss of mass of MMSP microspheres within a given temperature range was about 11.3% due to the removal of PEI molecules. The weight loss of GO sheets in this range due to the groups of COOH, OH, C = O, and epoxide was about 44.5%. [27] The combined analysis of these TGA results of the composites with each component indicated that the mass partition of the MMSP microspheres was about 7.5%, which was consistent with the reaction stoichiometry.

3.2. Investigation of Adsorption of Pb(II)/Cd(II) by MMSP-GO or MMSP

We performed batch adsorption experiments with Pb(II) and Cd(II) using MMSP-GO composites and MMSP microspheres. The adsorption capacities of Pb(II) and Cd(II) both increased as pH value increased, peaking at pH 9.0. The same trend was observed for each heavy metal ion. The adsorptive property of MMSP-GO composites was better than that of MMSP microspheres. This was because the GO nanosheets had a stronger absorptive ability than MMSP microspheres (Figure S1). For Pb(II) removal, the maximum adsorption at an equilibrium between MMSP-GO composites and MMSP microspheres was 220 and 152 mg g^{-1}, respectively, at an initial metal ion concentration of 20 mg L^{-1}. For Cd(II) removal, the maximum adsorption at equilibrium of MMSP-GO composites and MMSP microspheres was 65 and 23 mg g^{-1}, respectively (Figure 7). All results indicated that the composites containing GO were able to adsorb more heavy metal ions than those without GO. By comparison, the adsorptive capacity of Pb(II) was higher than that of Cd(II), which resulted from the increased utilization of amino groups on MMSP. [31] At the same time, GO has a greater saturation adsorptive capacity for Pb(II) than Cd(II). [32] It was reported that electrostatic interaction maybe the predominant driven force for adsorption of heavy metal ions by GO materials. [27] In this case, majority of Pb(II) and Cd(II) were adsorbed by GO sheets due to the electrostatic interaction between the GO with negative surface charges and cations in the broad pH range.

3.3. Adsorption Isotherms

Adsorption isotherm is important for determining the adsorption behavior of an adsorbent. Pb(II) and Cd(II) adsorption isotherm of MMSP-GO were investigated at pH 7.1. The

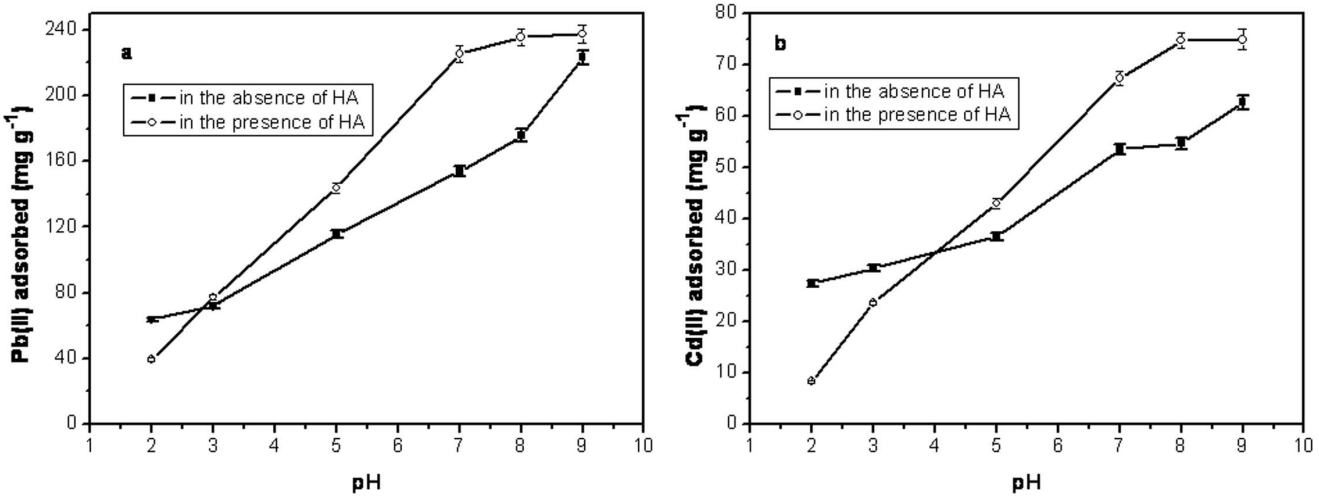

Figure 9. Effects of HA on the adsorption of heavy metal ions by the composites. Effects of HA on the adsorption of (a) Pb(II) and (b) Cd(II) on polyethylenimine-modified magnetic mesoporous silica and graphene oxide (MMSP-GO) composites.
doi:10.1371/journal.pone.0065634.g009

maximum Pb(II) and Cd(II) adsorption amounts on MMSP-GO within the tested concentration range in Figure 8. The equilibrium data were fitted by Langmuir and Freundlich model.

$$\text{Langmuir}: \frac{C_e}{q_e} = \frac{C_e}{q_{\max}} + \frac{1}{q_{\max} b} \quad (2)$$

$$\text{Freundlich}: \log q_e = \frac{\log C_e}{n} + \log k_f \quad (3)$$

where, q_{max} (mg g^{-1}) is the theoretical maximum heavy metals adsorption amounts, q_e (mg g^{-1}) is the equilibrium adsorption amount at heavy metals equilibrium concentration C_e (mg L^{--1}), where K_f is Freundlich coefficient characteristic of the adsorption affinity of the adsorbent, and n is the linearity index. The validity of isotherm models used in this study is assessed by correlation coefficient (R^2). The fitted results of all isotherm models were investigated in this study are presented in the Table S1. The results showed that Langmuir model with R^2 higher than 0.99 fitted better than Freundlich model, indicating that Pb(II) and Cd(II) adsorption on MMSP-GO can be considered to be a monolayer adsorption process. The abundant oxygen-containing functional groups on the surface of graphene oxide made the adjacent oxygen atoms available to bind metal ions [27]. At the same time, the amino groups of MMSP had a strong affinity towards metal ions, and the possible adsorption mechanism could be reasoned out by the coordinate interactions. [33].

3.4. Adsorption of Pb(II)/Cd(II) by MMSP-GO Influenced by HA

We also investigated the influence of HA at an initial concentration of 10 mg L^{--1} on the adsorption of heavy metal ions onto MMSP-GO composites within a pH range of 2.0 to 9.0. For both types of metal ions of Pb(II) and Cd(II), the adsorption capacity of the ion in the presence of HA was greater than in the absence of HA for MMSP-GO composites after a certain pH value (Figure 9). The two curves crossed at about pH 3.0 for Pb(II) and about pH 4.0 for Cd(II). Under pH neutral conditions, about 72 mg g^{-1} more Pb(II) was adsorbed in the presence of HA than in its absence, and about 14 mg g^{-1} more Cd(II) was adsorbed. The amounts HA adsorbed by MMSP-GO composites in the presence of Pb(II) or Cd(II) were about 83 and 87 mg g^{-1}, respectively, under neutral conditions. The adsorption capacity of HA molecules remained roughly the same no matter which heavy metal ions were present. This implied that there was a specific site for HA adsorption on the MMSP-GO and that this site was not influenced by metal ion adsorption. We reported previously that PEI-modified MMSP microspheres could adsorb HA molecules efficiently across a wide pH range. [28] Nanoparticles coated with HA showed enhanced adsorption of heavy metal ions, such as Pb(II).[34–37] As with GO nanosheets, at pH>7.0, adsorption of Cd(II)/Pb(II) was hindered by the presence of 10 mg L^{-1} HA in the solution because the HA would bind to the adsorbent, competing with the metal ions. [27] On the contrary, the enhanced adsorption of the metal ions onto MMSP-GO composites in the presence of HA molecules may be attributed to the joint effects of the PEI-modified MMSP microspheres and the GO sheet. When HA is not present during adsorption, the metal ions may have been mainly adsorbed onto GO nanosheets, accompanied by only some adsorption onto MMSP. In contrast, in the presence of HA, most of the HA was trapped by the MMSP microspheres, and so metal ions were able to interact with the HA on the composite surface. Moreover, adsorption of HA molecules could neutralize the positive surface charge of the MMSP and enhance adsorption of heavy metal ions. In this way, in addition to the adsorption of metal ions onto the GO surface, extra metal ions could be adsorbed onto MMSP microspheres mediated by HA on their surfaces. We examined the sorption of HA by the composites through FTIR measurements. Description of the major transmittance bands in FTIR spectra of HA, MMSP-GO composites, MMSP-GO/HA/Pb^{2+} and MMSP-GO/HA/Cd^{2+} complex are presented in Figure S2. By comparison with bulk HA and pure MMSP-GO composites, the strengthened peak intensity and occurrence of new peak of bands at 1580, 2700 and 3900 cm^{-1} diminished markedly for both MMSP-GO/HA/Pb^{2+} and MMSP-GO/HA/Cd^{2+}, which could result from the strong interactions of COOH, Phenolic OH, and OH of aliphatic alcohol with MMSP-GO composites. This result proved successful adsorption of HA by the composites.

Conclusions

A facile and reproducible method was developed and used to prepare magnetic mesoporous silica-graphene oxide composites (MMSP-GO) with hierarchical structures and unique properties. These composites were suitable for synergistic adsorption of heavy metal ions and humic acid molecules. The magnetic mesoporous silica microspheres were synthesized and functionalized with PEI molecules, which provided abundant amine groups for chemical conjugation with the carboxyl group on GO sheets and enhanced affinity between pollutants and the mesoporous silica. Adsorption results recorded under different conditions indicated that this experiment was sufficient to prove that this system was capable of simultaneous removal of heavy metal ion and humic acid using MMSP-GO composites as the adsorbent. The underlying mechanism of synergistic adsorption of heavy metal ions and humic acid were discussed. This kind of composite adsorbent was able ot make use of both the large specific surface area and surface functionalities of GO and mesoporous structures. This allowed them to efficiently adsorb the heavy metal ions and HA, and the adsorption of HA onto the composites enhanced the adsorption efficiency of Pb(II) and Cd(II).

Supporting Information

Figure S1 a. Effects of pH on adsorption of Pb(II) by MMSP and GO (Initial concentrations: 20 mg L^{-1}; adsorbent loading: 100 mg L^{-1}); b. Effects of pH on adsorption of Cd(II) by MMSP and GO (Initial concentrations: 20 mg L^{-1}; adsorbent loading: 100 mg L^{-1}).
(TIF)

Figure S2 FTIR spectra of bulk HA (a), MMSP-GO composites (b), MMSP-GO/HA/Pb(II) complex (c), and MMSP-GO/HA/Cd(II) complex (d).
(TIF)

Table S1 Constants and correlation coefficients of Pb(II) and Cd(II) adsorption by langmuir and Freundlich model.
(DOC)

Author Contributions

Conceived and designed the experiments: YLW YLT. Performed the experiments: YLW SL FFG YLT. Analyzed the data: YLW BDC SLY YLT. Contributed reagents/materials/analysis tools: YLW YLT. Wrote the paper: YLW YLT.

References

1. Prelot B, Einhorn V, Marchandeau F, Douillard J-M, Zajac J (2012) Bulk hydrolysis and solid-liquid sorption of heavy metals in multi-component aqueous suspensions containing porous inorganic solids: Are these mechanisms competitive or cooperative? Journal of Colloid and Interface Science 386: 300–306.
2. Zhang XG, Minear RA (2002) Characterization of high molecular weight disinfection byproducts resulting from chlorination of aquatic humic substances. Environmental Science & Technology 36: 4033–4038.
3. Campbell L, Dixon DG, Hecky RE (2003) A Review Of Mercury in Lake Victoria, East Africa: Implications for Human and Ecosystem Health. Journal of Toxicology and Environmental Health, Part B 6: 325–356.
4. Larraza I, López-Gónzalez M, Corrales T, Marcelo G (2012) Hybrid materials: Magnetite-Polyethylenimine-Montmorillonite, as magnetic adsorbents for Cr(VI) water treatment. Journal of Colloid and Interface Science 385: 24–33.
5. Guo J, Chen S, Liu L, Li B, Yang P, et al. (2012) Adsorption of dye from wastewater using chitosan-CTAB modified bentonites. Journal of Colloid and Interface Science 382: 61–66.
6. Hua M, Zhang S, Pan B, Zhang W, Lv L, et al. (2012) Heavy metal removal from water/wastewater by nanosized metal oxides: A review. Journal of Hazardous Materials 211–212: 317–331.
7. Jung JH, Lee JH, Shinkai S (2011) Functionalized magnetic nanoparticles as chemosensors and adsorbents for toxic metal ions in environmental and biological fields. Chemical Society Reviews 40: 4464–4474.
8. Zhang Y, Xu S, Luo Y, Pan S, Ding H, et al. (2011) Synthesis of mesoporous carbon capsules encapsulated with magnetite nanoparticles and their application in wastewater treatment. Journal of Materials Chemistry 21: 3664–3671.
9. Sun DD, Lee PF (2012) TiO_2 microsphere for the removal of humic acid from water: Complex surface adsorption mechanisms. Separation and Purification Technology 91: 30–37.
10. Yokoi T, Kubota Y, Tatsumi T (2012) Amino-functionalized mesoporous silica as base catalyst and adsorbent. Applied Catalysis a-General 421: 14–37.
11. Wang F, Tang Y, Zhang B, Chen B, Wang Y (2012) Preparation of novel magnetic hollow mesoporous silica microspheres and their efficient adsorption. Journal of Colloid and Interface Science 386: 129–134.
12. Walcarius A, Mercier L (2010) Mesoporous organosilica adsorbents: nanoengineered materials for removal of organic and inorganic pollutants. Journal of Materials Chemistry 20: 4478–4511.
13. Sierra I, Perez-Quintanilla D (2013) Heavy metal complexation on hybrid mesoporous silicas: an approach to analytical applications. Chemical Society Reviews, Advance Article. doi:10.1039/C2CS35221D.
14. Feng X, Fryxell GE, Wang LQ, Kim AY, Liu J, et al. (1997) Functionalized monolayers on ordered mesoporous supports. Science 276: 923–926.
15. Lam KF, Yeung KL, McKay G (2006) A rational approach in the design of selective mesoporous adsorbents. Langmuir 22: 9632–9641.
16. Lam KF, Chen XQ, McKay G, Yeung KL (2008) Anion Effect on Cu^{2+} Adsorption on NH_2-MCM-41. Industrial & Engineering Chemistry Research 47: 9376–9383.
17. Burleigh MC, Markowitz MA, Spector MS, Gaber BP (2001) Amine-functionalized periodic mesoporous organosilicas. Chemistry of Materials 13: 4760–4766.
18. Yoshitake H, Yokoi T, Tatsumi T (2002) Adsorption of chromate and arsenate by amino-functionalized MCM-41 and SBA-1. Chemistry of Materials 14: 4603–4610.
19. Liu AM, Hidajat K, Kawi S, Zhao DY (2000) A new class of hybrid mesoporous materials with functionalized organic monolayers for selective adsorption of heavy metal ions. Chemical Communications 0: 1145–1146.
20. Li GL, Zhao ZS, Liu JY, Jiang GB (2011) Effective heavy metal removal from aqueous systems by thiol functionalized magnetic mesoporous silica. Journal of Hazardous Materials 192: 277–283.
21. Yokoi T, Tatsumi T, Yoshitake H (2004) Fe^{3+} coordinated to amino-functionalized MCM-41: an adsorbent for the toxic oxyanions with high capacity, resistibility to inhibiting anions, and reusability after a simple treatment. Journal of Colloid and Interface Science 274: 451–457.
22. Chen XQ, Lam KF, Zhang QJ, Pan BC, Arruebo M, et al. (2009) Synthesis of Highly Selective Magnetic Mesoporous Adsorbent. Journal of Physical Chemistry C 113: 9804–9813.
23. Wang P, Lo IMC (2009) Synthesis of mesoporous magnetic gamma-Fe_2O_3 and its application to Cr(VI) removal from contaminated water. Water Research 43: 3727–3734.
24. Tokuyama H, Hisaeda J, Nii S, Sakohara S (2010) Removal of heavy metal ions and humic acid from aqueous solutions by co-adsorption onto thermosensitive polymers. Separation and Purification Technology 71: 83–88.
25. Yang SB, Hu J, Chen CL, Shao DD, Wang XK (2011) Mutual Effects of Pb(II) and Humic Acid Adsorption on Multiwalled Carbon Nanotubes/Polyacrylamide Composites from Aqueous Solutions. Environmental Science & Technology 45: 3621–3627.
26. Sheng GD, Li JX, Shao DD, Hu J, Chen CL, et al. (2010) Adsorption of copper(II) on multiwalled carbon nanotubes in the absence and presence of humic or fulvic acids. Journal of Hazardous Materials 178: 333–340.
27. Zhao GX, Li JX, Ren XM, Chen CL, Wang XK (2011) Few-Layered Graphene Oxide Nanosheets As Superior Sorbents for Heavy Metal Ion Pollution Management. Environmental Science & Technology 45: 10454–10462.
28. Tang YL, Liang S, Yu SL, Gao NY, Zhang J, et al. (2012) Enhanced adsorption of humic acid on amine functionalized magnetic mesoporous composite microspheres. Colloids and Surfaces a-Physicochemical and Engineering Aspects 406: 61–67.
29. Xu XQ, Deng CH, Gao MX, Yu WJ, Yang PY, et al. (2006) Synthesis of magnetic microspheres with immobilized metal ions for enrichment and direct determination of phosphopeptides by matrix-assisted laser desorption ionization mass spectrometry. Advanced Materials 18: 3289–3293.
30. Xu X, Song C, Andrésen JM, Miller BG, Scaroni AW (2003) Preparation and characterization of novel CO_2 "molecular basket" adsorbents based on polymer-modified mesoporous molecular sieve MCM-41. Microporous and Mesoporous Materials 62: 29–45.
31. Hao S, Zhong Y, Pepe F, Zhu W (2012) Adsorption of Pb^{2+} and Cu^{2+} on anionic surfactant-templated amino-functionalized mesoporous silicas. Chemical Engineering Journal 189–190: 160–167.
32. Deng XJ, Lu LL, Li HW, Luo F (2010) The adsorption properties of Pb(II) and Cd(II) on functionalized graphene prepared by electrolysis method. Journal of Hazardous Materials 183: 923–930.
33. Pang Y, Zeng GM, Tang L, Zhang Y, Liu YY, et al. (2011) PEI-grafted magnetic porous powder for highly effective adsorption of heavy metal ions. Desalination 281: 278–284.
34. Liu JF, Zhao ZS, Jiang GB (2008) Coating Fe_3O_4 Magnetic Nanoparticles with Humic Acid for High Efficient Removal of Heavy Metals in Water. Environmental Science & Technology 42: 6949–6954.
35. Chen QQ, Yin DQ, Zhu SJ, Hu XL (2012) Adsorption of cadmium(II) on humic acid coated titanium dioxide. Journal of Colloid and Interface Science 367: 241–248.
36. Wu PX, Zhang Q, Dai YP, Zhu NW, Dang Z, et al. (2011) Adsorption of Cu(II), Cd(II) and Cr(III) ions from aqueous solutions on humic acid modified Ca-montmorillonite. Geoderma 164: 215–219.
37. Lin JW, Zhan YH, Zhu ZL (2011) Adsorption characteristics of copper (II) ions from aqueous solution onto humic acid-immobilized surfactant-modified zeolite. Colloids and Surfaces a-Physicochemical and Engineering Aspects 384: 9–16.